COBEM 2021 26th International Congress of Mechanical Engineering
November 22-26, 2021, Virtual Congress, Brazil

COB-2021-1116
THERMODYNAMIC EVALUATION OF TWO PORTABLE COOLERS RUNNING WITH RECIPROCATING AND ROTARY COMPRESSORS

Diego Marchi
Christian J. L. Hermes
POLO Laboratories, Mechanical Engineering Department, Federal University of Santa Catarina, Florianópolis, SC, Brazil
marchi@polo.ufsc.br

Adriano F. Ronzoni
Nidec Global Appliance, 89219-521, Joinville, SC, Brazil

Abstract. *Small-capacity refrigeration has got an increasing attention of the consumer market. In addition to the efficiency of electric equipment, the demand for compactness has also become a relevant requirement. Among the alternatives available to cool down small cabinets, mechanical vapor compression refrigeration remains prominent due to its satisfactory performance when compared to other cooling technologies. Compressor industries have invested in the development of compact and efficient products, exploring different compression principles for small-capacity applications, as is the case of rotary compressors. In this context, the objective of the present work is to assess the thermodynamic performance of a 38-liter portable vapor compression refrigeration system running with two different compressors designed for small-capacity applications: rotary and reciprocating. Experimental tests were carried out at three different ambient temperatures (16, 25 and 32 °C) in order to obtain the key performance parameters for each compressor (e.g., power consumption, cooling capacity, internal air temperature, and the condensing and evaporating temperatures). Finally, thermodynamic analyses were conducted to account for the internal and external irreversibilities by means of second law efficiencies, allowing for a comparison of the system performance running with both compressors in the same thermodynamic grounds. Albeit a refrigeration (second law) efficiency by 25% higher was observed for the reciprocating compressor, it provided a smaller cooling capacity and, therefore, led to a higher pull-down time.*

Keywords: *thermodynamic efficiency, portable cooler, reciprocating compressor, rotary compressor*

1. INTRODUCTION

Either for carrying goods or cooling electronic devices, the demand for compact and efficient refrigeration systems has gained importance in modern times, paving the road towards refrigeration miniaturization. From the application standpoint, the recent issue of vaccine transportation and conservation demands compact refrigeration systems throughout the whole cold chain, from the manufacturer to the beneficiary (Kahn *et. al*, 2017). According to Coulomb (2021), nearly 40% of conventional vaccines are unusable due to the lack of a suitable cold chain. Among the technologies available to cool down compact cabinets, mechanical vapor compression refrigeration systems have gained attention mainly due to their attractiveness in terms of energy efficiency. Nonetheless, the tradeoff between size and efficiency is an essential design aspect of portable coolers, impelling the industry to develop increasingly smaller but efficient compressors (Ribeiro, 2012). There is nowadays a wide variety of compact compressors available for such purposes, with different performance levels and operating envelopes.

The present work is aimed at evaluating and comparing the thermodynamic performance of a portable refrigeration system running with two different compressors: rotary and reciprocating (crankshaft). Experimental tests were carried out at three different ambient temperatures (16, 25 and 32 °C) in order to obtain the key performance parameters for each compressor (e.g., power consumption, cooling capacity, compressor runtime, internal air temperature, and the condensing and evaporating temperatures). However, the direct comparison between the overall energy consumption may be unfair from a thermodynamic standpoint. Therefore, for comparisons purposes, the methodology introduced by Hermes and Barbosa (2012) – consisting of splitting the second law efficiency, also called the refrigeration efficiency, into two terms, one associated with internal losses (*e.g.*, friction, mixtures) and another with external losses (*e.g.*, heat transfer across finite temperature difference) – was adopted in the present paper, allowing for a comparison of the system performance running with both compressors in the same thermodynamic grounds.

2. EXPERIMENTAL WORK

The characteristics of the refrigeration system under analysis are summarized in Table 1. This portable cooler (available on the market) is comprised of a 38-liter cabinet and is originally equipped with a reciprocating compressor,

which operates with 42 g of HFC-134a. The heat rejection to the environment is performed by means of a fan-supplied tube-fin condenser, while the refrigerated compartment is cooled down by a roll-bond evaporator distributed along the internal walls. More details of the cooler and its heat exchangers are illustrated in Figure 1.

Table 1. Baseline system characteristics.

Overview	Parameter	Value
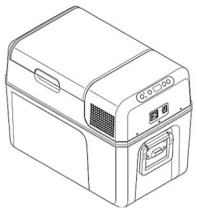	Cabinet Volume, liter	38
	Energy Consumption, kWh/annum	102
	Energy Efficiency class (EU)	A+
	Storage Temperature Range, °C	-10 to 10
	Noise Emission, dB(A)	49
	Weight, kg	11.2
	Ambient Temperature, °C	16, 25, 32
	Evaporator	Roll-bond, natural draft
	Condenser	Air source, forced draft

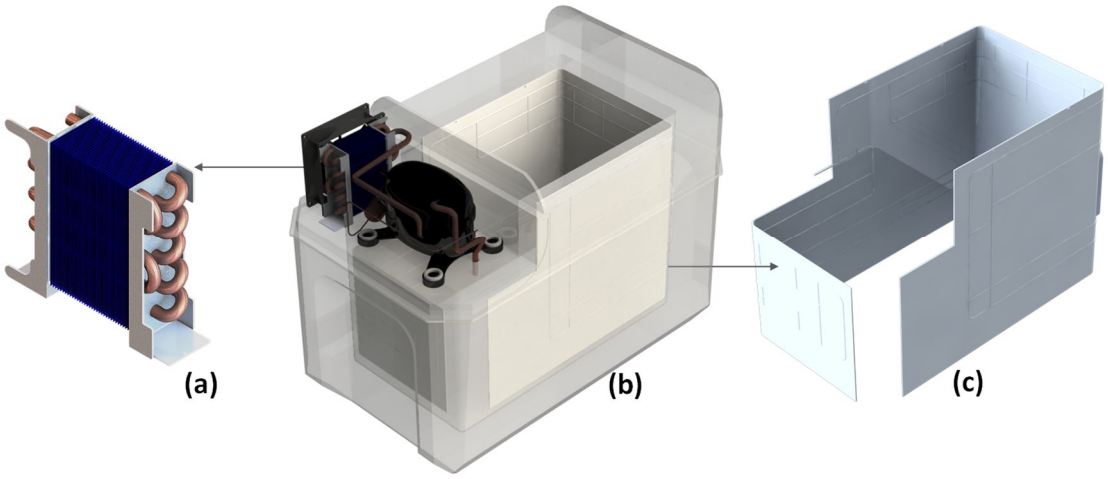

Figure 1. Portable cooler under analysis: (a) condenser, (b) refrigerated cabinet, (c) evaporator.

The compressors analyzed in this work are described in Table 2. On the one hand, the baseline compressor present in the original system design is a fixed speed reciprocating (crankshaft) compressor which operates at 60 Hz. On the other hand, a prospective replacement is a miniature rotary type compressor with two compression stages. This compression technology is usually adopted in air conditioning applications, as it presents low efficiencies at low evaporating temperatures. Nonetheless, according to manufacturer's data, such a compressor can operate in a wide range of evaporating temperatures spanning both cooler and freezer applications. The rotary compressor was evaluated at two speeds, 40 and 58 Hz, far from the operating thresholds.

Table 2. Compressor data.

Compressor	Reciprocating	Mini-rotary
Evaporating temperature range, °C	-35 to 0	-30 to 20
COP LBP, W/W	0.89	1.11
Stroke, cm³	1.3	2.4
Mass, kg	2.3	1.2
Dimensions: $H \mid L \mid W$, mm	159 | 149 | 154	154 | 77 | 107
External shell volume, liter	1.03	1.2
Frequency range, Hz	not informed	20 to 80

Experimental tests were carried out in a climate chamber with strict control of temperature, humidity and air speed. Temperature at several points in the refrigeration loop were measured using T-type thermocouples with a measurement uncertainty of ±0.2°C. The average air temperature inside the refrigerated compartment was obtained from 9 thermocouples, five of which positioned in the horizontal medium plane, as shown in Figure 2. The thermocouples used for measuring the cabinet air temperatures were brazed in cylindrical copper blocks, following the recommendations of the ISO/FDIS 15502 (2005) standard. All the surface thermocouples employed a thin electrical insulation medium between the thermocouple and the surfaces to avoid undesired electrical noise.

The surrounding air temperature was measured in three different positions around the cabinet (front, right and back). The condensing and evaporating temperatures were obtained through surface thermocouples placed on the refrigerant piping in the middle of the heat exchangers. The instantaneous power consumption was measured during the tests through a digital analyzer with an uncertainty of ±0.1% of the full scale, while the power consumed by other components, such as fan and control boards were evaluated beforehand.

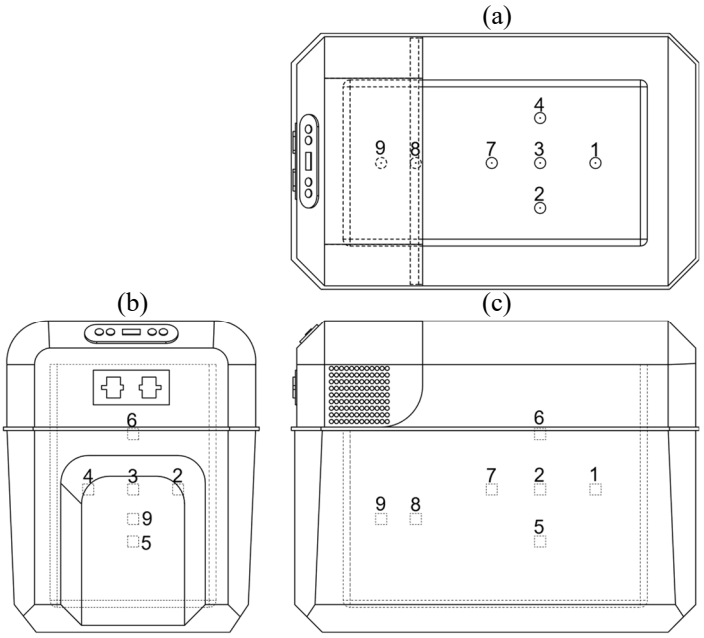

Figure 2. Schematic of cabinet air temperature instrumentation: (a) top view, (b) front view and (c) side view.

In the present study, the overall thermal conductance of the cabinet was estimated based on a reverse heat flux test (Vineyard *et al.*, 1998), according to which the internal temperatures are maintained above surrounding air temperature by means of heat dissipation inside the refrigerated compartment via electrical heaters, as depicted in Fig. 3. During the test, the refrigeration system is switched off and the air temperatures inside and outside the cabinet are monitored, along with the power consumed by the heaters. The thermal conductance of the cabinet can then be calculated at steady-state condition using the following energy balance:

$$UA_{cab} = \frac{\dot{W}_{res}}{T_i - T_e} \tag{1}$$

where UA_{cab} represents the overall cabinet conductance (=0.52 W/K), $\dot{W}_{res}$ is the mean power dissipated by the heaters in W, T_i is the cabinet internal temperature and T_e the surrounding air temperature.

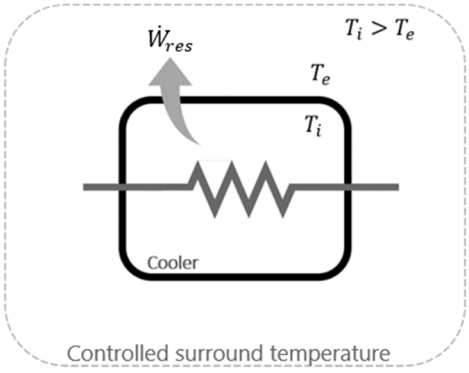

Figure 3. Cabinet reverse heat leakage test scheme.

The thermodynamic performance of the refrigerator was experimentally evaluated through pull-down tests and steady-state energy consumption tests (Hermes et al., 2013). For the pull-down tests, the refrigerator is kept with the door open

inside the climate chamber at 25 °C until the thermal equilibrium is reached. At this point, the door is closed and the refrigeration system is switched on at its maximum cooling capacity. The pull-down test consists of monitoring the temperatures, pressures and power consumption of the system from the compressor start until the steady-state is reached.

For the energy consumption tests, electric heaters were installed within the refrigerated compartment to maintain the storage temperature fixed, which was done by means of a PID controller (Proportional-Integral-Derivative). Thus, the refrigerator operates at steady-state condition with the compressor running continuously. The compressor runtime ratio (RTR) is, therefore, calculated from (Hermes et al., 2013) $RTR = \dot{Q}_t/\dot{Q}_e$, where $\dot{Q}_t = UA_{cab}(T_e - T_i)$ is the cabinet thermal load and $\dot{Q}_e = \dot{Q}_t + \dot{W}_{res}$ is the cooling capacity of the refrigeration system, where $\dot{W}_{res}$ is the power dissipated by the heaters. The energy consumption is obtained from $CE = \text{RTR}\sum \dot{W}$, where $\sum \dot{W}$ accounts for the overall power consumption of the system (compressor, condenser fan, control board). For both compressors, the tests were performed under three different surrounding air temperatures (16, 25 and 32°C), with three distinct cabinet internal temperatures (-4, 0 and 4 °C), as illustrated in Figure 4.

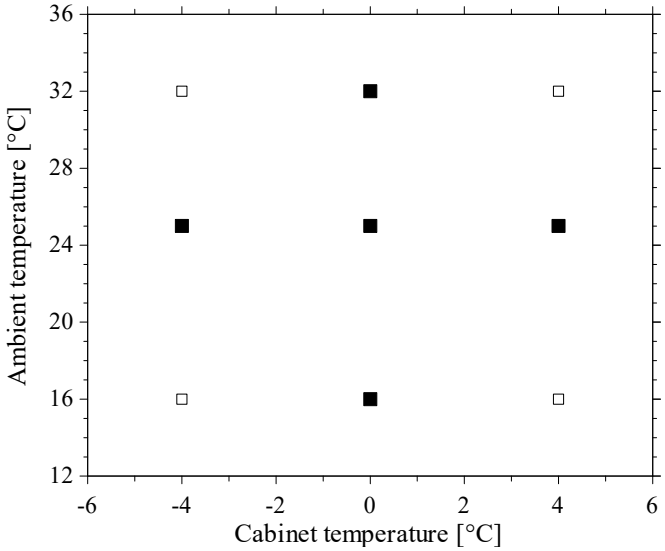

Figure 4. Experimental conditions

In the present study, a total of 18 experimental tests were carried out (15 steady-state + 3 pull-down). The slope of the trends for each variable, in each interval of 30 min, needs to be less than two standard deviations for steady-state condition be established. Once this condition was reached, the values for each variable were evaluated from its mean value, with a standard deviation below ±1% for power and pressures, and ±0.2°C for temperatures. In addition, uncertainty values were derived for each variable yielding ±0.5°C for temperatures and ±1 W for power consumption and cooling capacity.

3. THERMODYNAMIC MAPPING

According to Gosney (1982), the coefficient of performance of a real refrigeration system is defined by the ratio between the cooling capacity and the overall power consumption, yielding:

$$COP_{real} = \frac{\dot{Q}_e}{\sum \dot{W}} \tag{2}$$

The coefficient of performance of an ideal refrigerator running under the so-called Carnot cycle, where all the thermodynamic processes are considered reversible, depends only of the cabinet and surrounding temperatures, yielding:

$$COP_{ideal} = \frac{T_i}{T_e - T_i} \tag{3}$$

where $T_i < T_e$. Moreover, assuming that the refrigeration system operates ideally between the hot (T_h) and cold (T_c) ends (see Fig. 5), the following expression for the COP of a so-called endoreversible refrigerator is obtained from:

$$COP_{endo} = \frac{T_i - \Delta T_c}{T_e - T_i + \Delta T_h + \Delta T_c} \tag{4}$$

where ΔT_h and ΔT_c represent the temperature differences at the hot and cold ends, respectively. It is important to point out that the endorreversible coefficient of performance is the maximum COP possible for an ideal refrigeration system running with real heat exchangers, that is, with a finite temperature difference between the terminals and the reservoirs. It should be noted that once $\Delta T \rightarrow 0$, thus $COP_{endo} \rightarrow COP_{ideal}$.

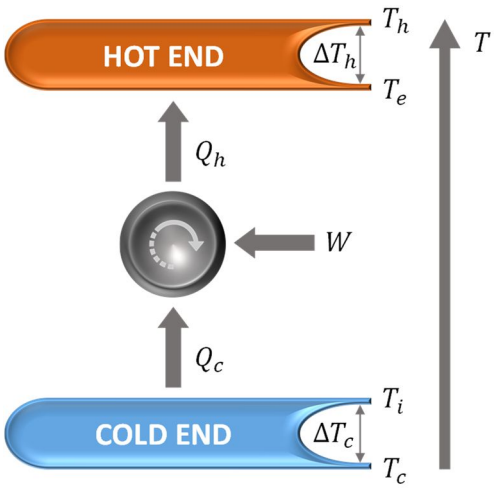

Figure 5. Thermodynamic representation of a refrigeration system

The second-law efficiency associated with the cycle internal irreversibilities can be calculated by comparing the performance coefficients of the real refrigerator and the endorreversible refrigerator, as follows:

$$\eta_{int} = \frac{COP_{real}}{COP_{endo}} \tag{5}$$

Similarly, the efficiency associated with external irreversibilities is calculated from:

$$\eta_{ext} = \frac{COP_{endo}}{COP_{ideal}} \tag{6}$$

Hence, the second-law efficiency of the refrigeration system is obtained from:

$$\eta_{2nd} = \frac{COP_{real}}{COP_{ideal}} = \eta_{int}\eta_{ext} \tag{7}$$

This approach is able to point out, through quantitative indicators, the key irreversibilities taking place in the refrigeration system.

4. RESULTS

Fig. 6 illustrates the results of the pull-down tests for the system operating with the original (reciprocating) and the rotary compressor running at 40 and 58 Hz for a surrounding air temperature of 25°C. It is possible to verify that, on the one hand, the system running with the reciprocating compressor reaches a steady-state temperature of approximately -15°C after 5.5 h. On the other hands, the system running with the rotary compressor running at 40 Hz takes approximately 5 h to reach -22 °C, whereas running at 58 Hz it reaches -27 °C after 4.5 h. Figure 6b shows the evolution of the overall power consumption, where power peaks are verified at the early stages in all cases. At steady-state, the system with the rotary compressor operating at 40 Hz presented a power consumption approximately 70 % higher than the baseline system, while running at 58 Hz, it drained twice as much as the power of the baseline system.

The steady-state test results are summarized in Table 3 in terms of indoor and outdoor temperatures, condensing and evaporating temperatures, as well as power consumption and cooling capacity. It should be noted that all systems were able to reach the specified conditions, indicating an excess of cooling capacity in comparison to the thermal load. Analyzing the temperature differences in the heat exchangers (*i.e.*, condenser and evaporator), the baseline system presented an average ΔT of around 8 °C on both heat exchangers. On the cold end, the rotary compressor showed an evaporation temperature 4°C and 12°C lower than the baseline at 40 Hz and 58 Hz operation, respectively. On the hot

end, the rotary compressor showed a condensing temperature 8°C and 14°C above the baseline at 40 Hz and 58 Hz operation, respectively. This can be explained mainly by the substantial increase in refrigerant mass flow rate provided by the rotary compressor compared to the baseline, which increases the evaporator cooling capacity and the condenser heat duty. In both cases, there are strong indications that the thermal sizes (number of transfer units) of the heat exchangers are too small to operate with the rotary compressor.

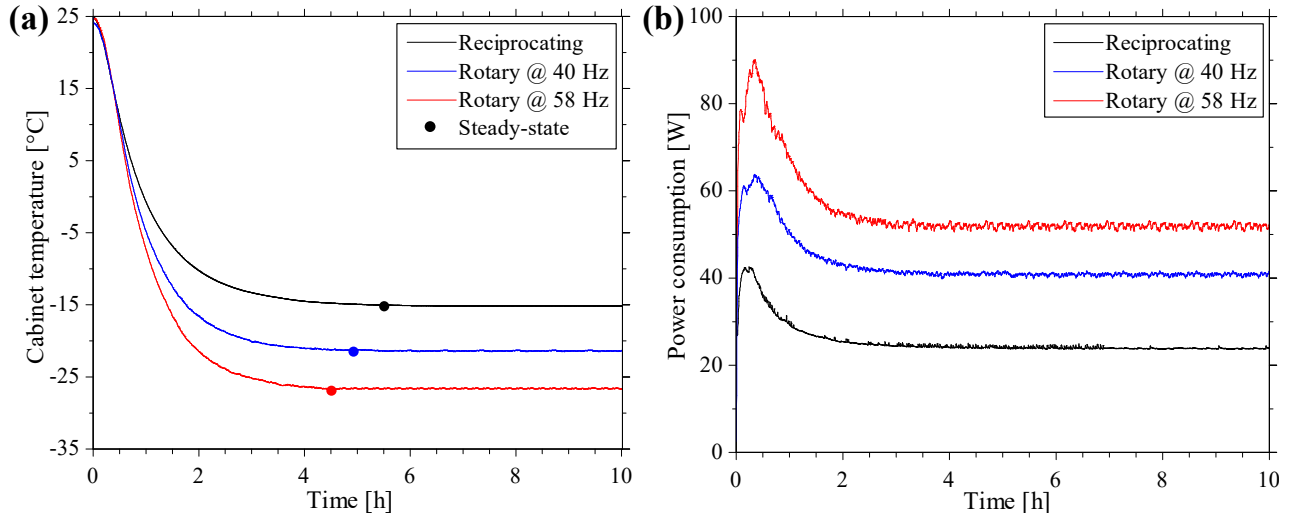

Figure 6. Pull-down test results: (a) cabinet temperature, and (b) power consumption.

Also, one can see in tests 2, 3 and 4 of Tab. 3, where the surrounding air temperature is held constant at 25 °C, that cooling capacity increases with the cabinet temperature, which is mainly due to the increase of the mass flow rate of refrigerant with the evaporating temperature. The effect of ambient temperature can be verified comparing tests 1 and 5, where the cabinet temperature is held constant at 0°C while the surrounding air temperature is changed from 16 to 32°C. A ~20% increase in the power consumption for a temperature span of 16 °C, and a ~25% reduction in the cooling capacity can also be observed in Tab. 3, which are mainly due to an increase in the condensing temperature, which reduces the specific refrigerant effect, increases the specific compression work and also reduces the refrigerant mass flow rate. It should be noted that the rotary compressor provided a cooling capacity by twice higher than that of the baseline system, albeit consuming much more power, thus affecting the system COP, as depicted in Fig. 7. One can note that the configuration A presented a better COP_{real} for all test conditions, despite having a lower cooling capacity, whilst configurations B and C showed figures 11% and 20% lower than the baseline.

Table 3. Summary of steady-state test results.

System	**A: Reciprocating**					**B: Rotary at 40 Hz**					**C: Rotary at 58 Hz**				
Test index	1	2	3	4	5	1	2	3	4	5	1	2	3	4	5
Ambient temp., °C	16.0	25.4	25.4	25.9	32.1	16.0	25.2	25.0	25.1	31.9	16.0	25.0	25.3	25.2	32.0
Cabinet temp., °C	-0.4	-4.3	-0.8	3.2	0.7	-0.1	-4.1	0.0	3.9	0.0	-0.2	-4.1	0.2	4.0	0.0
Evap. temp., °C	-10.2	-11.8	-9.3	-6.5	-7.1	-13.3	-14.8	-11.8	-9.4	-11.1	-14.9	-16.1	-13.0	-10.2	-13.0
Cond. temp. °C	24.8	32.0	32.7	33.5	40.7	32.6	40.2	41.8	42.4	48.1	37.5	44.5	49.0	49.4	52.8
Power input, W	28,1	28,6	29,7	31,4	30,7	50.0	53.4	57.2	58.9	61.3	70.3	73.1	79.3	85.6	80.8
Cooling cap., W	37,0	29,2	32,4	37,6	30,2	59.8	50.0	56.8	59.7	49.7	75.1	62.2	75.5	79.9	56.3

Also, Fig. 7 shows the COP values for the ideal and endoreversible conditions. In all cases, similar COP_{ideal} figures have been observed, reflecting the small variations due to the controls of the surrounding and cabinet temperatures. However, the inspection of Fig. 7 reveals that the COP_{endo} presented the most significant variations, where configurations B and C showed 23% and 32% lower figures than the baseline. As expected, the $COPs$ increase with the cabinet temperature (Fig. 7b), while decrease as the surrounding air temperature raises (Fig. 7a). Such results can be better explained with the help of the second law efficiencies, as depicted in Fig. 8. One can observe that the baseline system presented an overall efficiency 14% and 22% higher than configurations B and C, respectively, reflecting the gains in the COP_{real} as the COP_{ideal} figures remained fairly constant. Fig. 8 also reveals that notwithstanding the baseline system has higher external efficiencies in comparison to the one operating with the rotary compressor (configurations B and C) – reflecting the fact that the latter presented very high temperature differences in the condenser and the evaporator, thus increasing the external irreversibilities – the trends observed for the internal efficiencies are quite the opposite, with the

systems with the rotary compressor showing better figures than the baseline regardless the working conditions. This is so as the rotary compressor is notoriously more efficient than the reciprocating one.

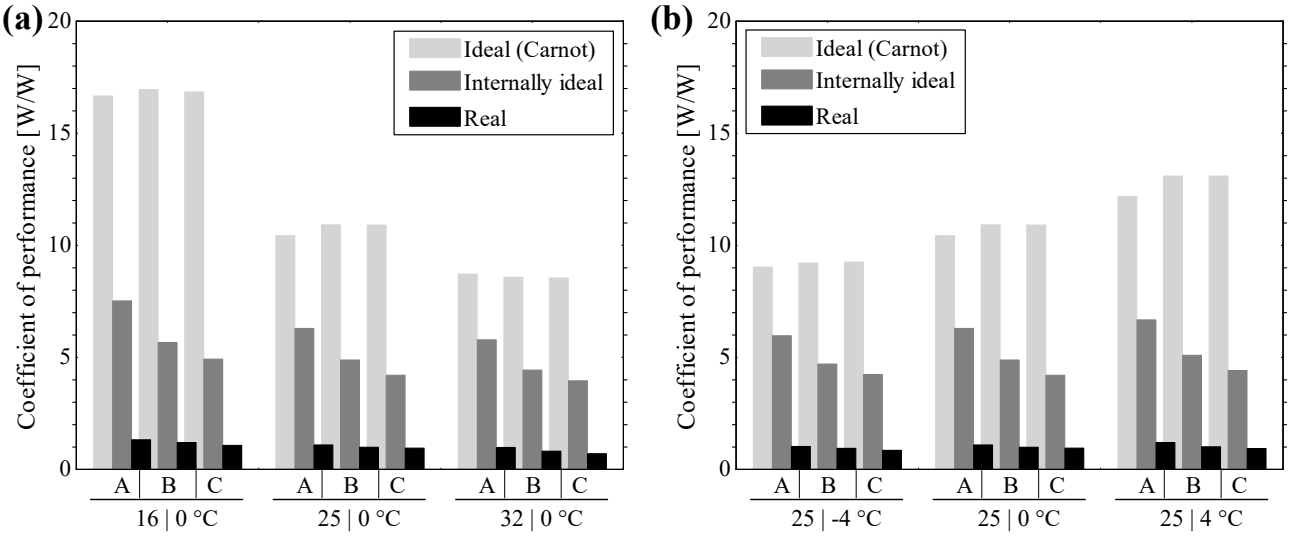

Figure 7. Coefficient of performance: (a) Cabinet temperature at 0°C and (b) Ambient temperature at 25°C (A: Reciprocating compressor, B: Rotary at 40 Hz, and C: Rotary at 58 Hz)

Finally, the analyses indicate that a proper dimensioning of the heat exchangers for operation with the rotary compressor could significantly improve the system performance as its internal efficiency is higher than that of the baseline. As the rotary compressor provides higher mass flow rate levels and consequently higher heat duties, it requires heat exchangers with larger number of transfer units to work efficiently. However, it is worth of note that the rotary compressor presents several concerns regarding to the oil return, such as pipeline limitation and compressor positioning, which ought to be taken into account in the case of a new system design.

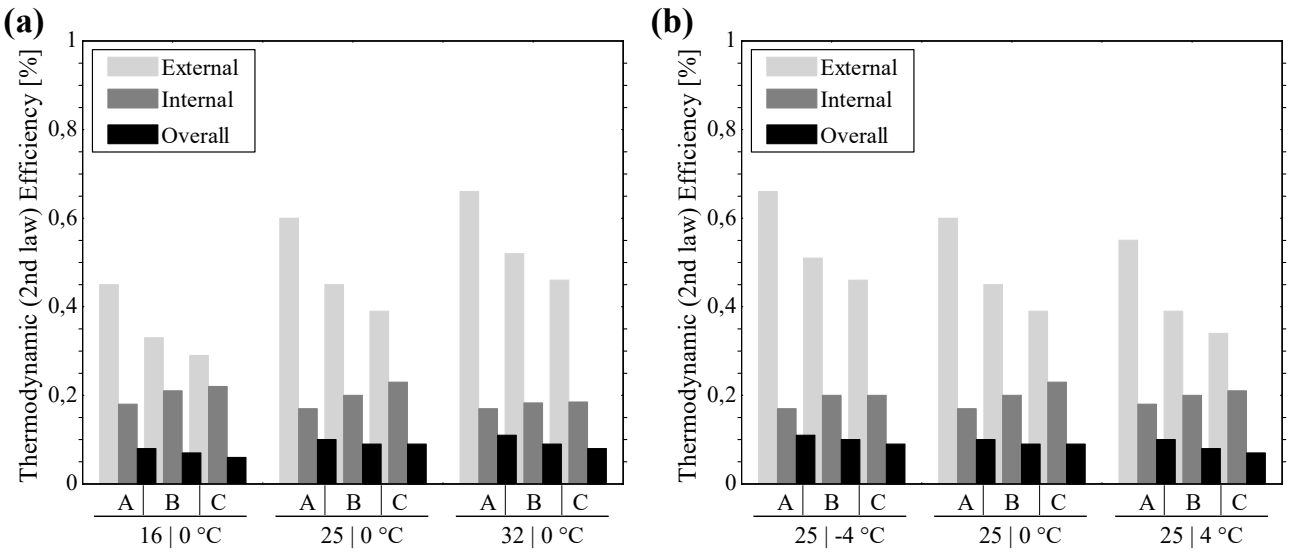

Figure 8. Second law efficiency: (a) Cabinet temperature at 0°C and (b) Ambient temperature at 25°C (A: Reciprocating compressor, B: Rotary at 40 Hz, and C: Rotary at 58 Hz)

5. CONCLUSIONS

A methodology for the thermodynamic comparison of a compact cooler operating with a reciprocating and a rotary compressor was employed in this work. Three configurations have been analyzed, namely A: the baseline system operating with a reciprocating compressor; B: the same system operating with a rotary compressor at 40 Hz; and C: the very system operating with a rotary compressor at 58 Hz. Experimental tests have been conducted at three controlled

levels of surrounding temperature (16, 25 and 32°C) and at three levels of cabinet temperature (-4, 0 and 4°C) in a rigorous controlled climate chamber. The operating parameters of each system were accounted for to derive the key performance parameters to quantify the internal and external irreversibilities of the refrigeration system. The baseline showed higher efficiency values, roughly 20 % higher than those observed for the system running with the rotary compressor. Albeit the compressor was the only component modified, the external efficiencies of configurations with the rotary compressor presented figures for the internal efficiency slightly than those of the baseline, thus indicating that a proper heat exchanger design should significantly improve the performance of the cooler for operation with the rotary compressor.

6. ACKNOWLEDGEMENTS

This work was conducted under the auspices of the National Institutes of Science and Technology (CNPq 404023/2019-3, FAPESC 2019TR0846). The authors are grateful for the financial support of Nidec/Embraco and Embrapii through grant No. PPOL-1901.0020.

7. REFERENCES

Coulomb D., 2021. “No refrigeration, no vaccination”. *International Journal of Refrigeration*, Editorial, Volume 123, pp. iv-v, ISSN 0140-7007, https://doi.org/10.1016/j.ijrefrig.2021.01.017.

Gonçalves, J. M., *et al.,* 2011. “Experimental Mapping of the Thermodynamic Losses in Vapor Compression Refrigeration Systems” *Journal of the Brazilian Society of Mechanical Sciences and Engineering,* Vol. 33, No. 2, pp. 159-165.

Gosney, W. B., 1982. *Principle of refrigeration.* Cambridge University Press, Cambridge, UK.

Hermes, C. J. L., Barbosa, J. R., 2012. “Thermodynamic comparison of Peltier, Stirling, and vapor compression portable coolers” *Applied Energy,* Vol. 91, No. 1, pp. 51-58.

Hermes, C.J.L., Melo, C., Knabben, F.T., 2013, “Alternative test method to assess the energy performance of frost-free refrigerating appliances”, *Applied Thermal Engineering*, Vol. 50, pp. 1029-1034.

ISOGUM, 2008. “Avaliação de dados de medição — Guia para a expressão de incerteza de medição (em português)”. *Joint Committee for Guides in Metrology (JCGM 100:2008).*

ISO/FDIS 15502, 2005, “Household refrigerating appliances – characteristics and test methods”, *International Organization for Standardization*, Geneva, Switzerland.

Kahn, A. L., Kristensen, D. and Rao, R., 2017. “Extending supply chains and improving immunization coverage and equity through controlled temperature chain use of vaccines,” *Vaccine*, Vol. 35, No. 17. Elsevier Ltd, pp. 2214–2216.

Ribeiro, G. B. 2012. "Development and analysis of a compact cooling system using the microcompressor," *13th InterSociety Conference on Thermal and Thermomechanical Phenomena in Electronic Systems in San Diego, United State of America 30 May - 1 June, 2012.* Institute of Electrical and Electronic Engineers. pp. 717-722.

Vineyard, E.A., Therese, K.S., Kenneth, E.W., Kenneth, W.C., 1998. “Superinsulation in refrigerators and freezers”, *ASHRAE Transactions*, Vol. 104, No. 2, pp. 1126-1134.

8. RESPONSIBILITY NOTICE

The authors are the only responsible for the printed material included in this paper.